water

MDPI

Article

A Study on Chemical Oxygen Demand (COD) Concentration Distribution and Its Hydrodynamic Mechanisms in Liaodong Bay, China

Xincang Liu [1,2], Jiahui Deng [1,2], Lianjie Zhang [1,2], Ping Wang [1,2,*], Guangshuai Zhang [1,2], Xiangke Dong [1,2] and Jiawen Sun [1,2]

[1] National Marine Environmental Monitoring Center, Dalian 116023, China; xcliu@nmemc.org.cn (X.L.); djhdut@163.com (J.D.); ljzhang@nmemc.org.cn (L.Z.); gszhang@nmemc.org.cn (G.Z.); xkdong@nmemc.org.cn (X.D.); jwsun@nmemc.org.cn (J.S.)

[2] State Environmental Protection Key Laboratory of Marine Ecological Environment Remediation, Dalian 116023, China

* Correspondence: wangping@nmemc.org.cn

Abstract: In order to reveal the impact of hydrodynamic conditions on the transport and diffusion of pollutants in Liaodong Bay in China, this article uses MIKE21 to establish a numerical model to simulate the hydrodynamic mechanisms of tidal currents and residual currents in Liaodong Bay. The model has been calibrated using observation data from 10 stations, and the simulation results of the tidal currents, Euler residual currents, Lagrangian residual currents, and particle tracking in Liaodong Bay have been calculated. Subsequently, a comparative analysis is conducted based on the abovementioned data and measured data, exploring the impact of hydrodynamic conditions on the transport and diffusion of COD in Liaodong Bay. The research results in this article indicate that high concentration COD areas are mainly concentrated in the coastal areas around the estuary of the Liao River and the Daliao River, and river input is the main source of COD in Liaodong Bay. The Euler residual circulation can form COD enrichment in some areas, which is significantly higher than the background concentration, and the large-scale transportation of COD after entering Liaodong Bay is determined by the Lagrangian residual current. The particle tracking results in the estuarine area can effectively characterize the actual transportation of pollutants. The results of the Lagrangian residual flow and particle tracking in the bay indicate that river pollutants are mainly transported to the west bank after entering Liaodong Bay. The distribution of a COD concentration of 1.5 mg/L confirms this finding. The research findings presented in this paper offer valuable insights into the spatial distribution and transportation mechanisms of pollutants. These results hold significant implications for pollution prevention and mitigation strategies in comparable bay environments.

Keywords: COD; Liaodong Bay; Eulerian residual current; Lagrangian residual current; particle tracking; MIKE21

check for updates

Citation: Liu, X.; Deng, J.; Zhang, L.; Wang, P.; Zhang, G.; Dong, X.; Sun, J. A Study on Chemical Oxygen Demand (COD) Concentration Distribution and Its Hydrodynamic Mechanisms in Liaodong Bay, China. *Water* **2024**, *16*, 2135. https://doi.org/10.3390/w16152135

Academic Editors: Helena M. Ramos, Juan Antonio Rodríguez Díaz and Jorge Matos

Received: 5 June 2024
Revised: 17 July 2024
Accepted: 24 July 2024
Published: 28 July 2024

Copyright: © 2024 by the authors. Licensee MDPI, Basel, Switzerland. This article is an open access article distributed under the terms and conditions of the Creative Commons Attribution (CC BY) license (https://creativecommons.org/licenses/by/4.0/).

1. Introduction

Bays are formed by the concave part of the coastline, and the twists and turns in the coastline lead to the widespread existence of bays at the sea–land boundary. Due to the shallow water depth, the low disturbance from wind and waves, and calm water bodies, bays have become an important base for humans to engage in marine-related economic activities and have helped to develop tourism. At the same time, high-intensity human activities continue to damage the ecological environment of bays, and the accelerating industrialization process and gradually increasing population have led to an increasing number of pollutants being generated [1]. These pollutants are discharged into the sea through rivers and sewage outlets, leading to the deterioration of seawater quality year by year [2]. Marine disasters, such as red tides and algal blooms [3–6], occur frequently.

This issue is particularly prominent in developing countries, such as China, especially in semi-enclosed bays, such as Liaodong Bay [6,7], which have shallow water depths and poor water exchange capacity.

The water quality (WQ) of the sea is the core component of the ecological environment quality in bays. If the water quality in the bay is severely polluted all year round, human activities that rely on the bay will be affected. Therefore, seeking effective solutions is crucial. On the one hand, practical actions should be taken, including the formulation of national water quality criteria [8,9] to constrain and limit the amount of major pollutants [10], seawater quality monitoring should be carried out [11], and targeted protection and remediation efforts should take place [12]. On the other hand, theoretical research should be conducted on the hydrodynamic and material transportation [13] in bays, in order to understand the transportation process of pollutants in seawater and the pollution mechanism of bays, guiding the development of governance measures.

Liaodong Bay is located in the northeastern part of the Bohai Sea in China. With an average water depth of 22 m and a total area of 30,597 km^2 [14,15], it is the northernmost semi-enclosed bay in China in terms of latitude [16]. Furthermore, it represents one of the most significant estuarine ecosystems in northern China [17] (Figure 1). Economically developed cities, such as Dalian, Yingkou, Panjin, Jinzhou, and Huludao, are distributed around Liaodong Bay [18]. The water in the bay has been severely polluted [19,20], and the complex diffusion of high-intensity pollution emissions driven by the tidal current field in the bay has made it very difficult to solve the water quality problem. Many studies have been conducted on the distribution of nutrients, the river input, and the nitrogen–phosphorus ratio (N/P) impact on eutrophication in Liaodong Bay and the Bohai Sea area [21,22], as well as the distribution and sources of heavy metals in sediment in key areas [23,24], the spatial distribution of pollutants, and the environmental risks [25,26]. However, the understanding of how the transport of pollutants (COD) in the bay is affected by hydrodynamic forces is still lacking.

This paper establishes a numerical model of the entire Bohai Sea, including Liaodong Bay; the model was validated by measured data from 10 tidal current stations. On the basis of the calculated tidal current (TC) field, the Euler residual current (ERC), Lagrange residual current (LRC), and particle tracking (PT) were calculated. Then, the distribution of COD in the bay during the same period was analyzed in comparison to the above calculated results, and the hydrodynamic mechanism of the COD concentration distribution in Liaodong Bay was explained. The conclusion of this article is of great significance for the prevention and control of pollution in bays mainly affected by river inputs, such as the formulation of water quality standards and criteria for various regions of the bay, and the preparation of marine environment protection plans.

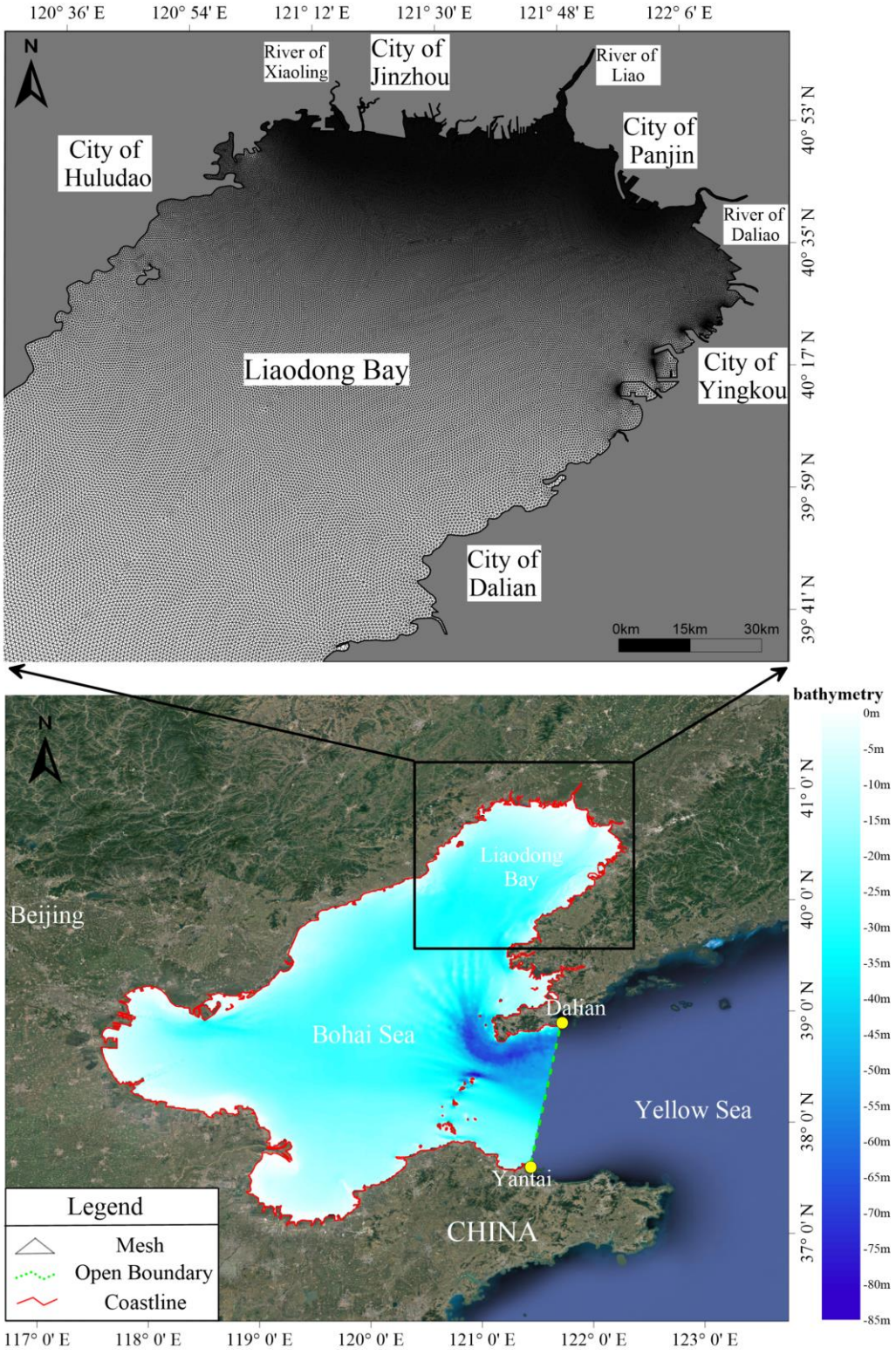

Figure 1. Study area and computational grid.

2. Numerical Model and Monitoring Data

2.1. Numerical Model

In this paper, the two-dimensional numerical model MIKE21, developed by the Danish Hydraulic Institute, is used for modeling. Its user-friendly interface and flexible unstructured grid system mean that it is widely used in numerical simulations of rivers, oceans, and lakes. The model covers the entire Bohai Sea, with coordinates ranging from 117.53 E

to 122.34 E and 37.02 N to 41.09 N. The model uses a triangular grid to dissect the computational domain and reduces the grid scale of Liaodong Bay. The side length of the smallest grid is about 50 m. The open boundary of the model, which is dictated by the water-level boundary, is the straight line connecting the Yantai and Dalian harbors. The water-level data are obtained from the Tide Table published by the National Marine Information Center and are inputted into the model as the open boundary after the datum adjustment. The water-depth data used here are based on the digitized nautical chart published by the Navigation Guarantee Department of the Chinese Navy Headquarters and the digital nautical chart of the DHI C-MAP. Liaodong Bay is mainly affected by periodic tidal currents, so this paper mainly studies the distribution characteristics of COD under tidal currents. In order to make the conclusion universal, factors with strong regional or irregular spatiotemporal features, like temperature, salinity, and meteorological variables, are not considered here.

2.2. Eulerian and Lagrangian Residual Currents

The ERC is the average of the tidal velocity field, which can be defined as [27]:

$$v_E = \frac{1}{T}\int_0^T \vec{v}\,\mathrm{d}t \tag{1}$$

In this paper, the calculation is performed according to the following equation:

$$v_E = \frac{1}{N}\sum_{i=1}^{N} \vec{v} \tag{2}$$

where v_E is the ERC on the current grid; $N = \frac{T}{\Delta t}$; N is the number of computation time steps; and T is the computation time, totaling 750 h, which can encompass the COD observation period and is an integer multiple of the tidal cycle. Δt is the computation time step and $\vec{v}$ is the TC on the grid.

Stokes drift (SD) represents the net mass transport resulting from the asymmetry between flood and ebb tidal currents, and can be defined as [27]:

$$v_S = \frac{1}{T\cdot D}\int_0^T \vec{v}\cdot\xi\,\mathrm{d}t \tag{3}$$

In this paper, the calculation is performed according to the following equation:

$$v_S = \frac{1}{N\cdot D}\sum_{i=1}^{N} \vec{v}\cdot\xi \tag{4}$$

where D is the distance from the mean sea level to the sea floor and ξ is the water surface elevation above the mean sea level.

The LRC is the average of the tidal flux field, which can be expressed as the vector sum of the ERC and SD [27], so the LRC v_L on the grid can be expressed as:

$$v_L = \frac{1}{N\cdot D}\sum_{i=1}^{N} \vec{v}\cdot\xi + \frac{1}{N}\sum_{i=1}^{N} \vec{v} \tag{5}$$

2.3. Particle Tracking Model

The particle tracking (PT) model calculates the transportation of dissolved, suspended, and sedimented substances discharged or accidently spilled into lakes, estuaries, coastal areas, and at open sea. The PT model can be used to calculate the transportation direction and distance of COD in Liaodong Bay under tidal currents, which is helpful to understand the influence of hydrodynamic mechanisms on the COD concentration distribution, and the equation can be expressed as [28]:

$$\begin{cases} \mathrm{d}x(t) = U(x,y,t)\mathrm{d}t + \mathrm{d}x'(t) \\ \mathrm{d}y(t) = V(x,y,t)\mathrm{d}t + \mathrm{d}y'(t) \end{cases} \tag{6}$$

where dx and dy are the displacement in the x and y directions, respectively. Moreover, d$x'(t)$ and d$y'(t)$ are the random walk displacements due to horizontal turbulent diffusion. The zonal (U) and meridional (V) components of the current velocity $\vec{v}$ are derived from numerical simulations. When particles reach open boundaries, they exit the computational domain and cease to participate in subsequent calculations. Upon reaching the coastline, particles are reflected back into the computational domain. The direction and velocity of this reflection are computed based on the incident angle of the particles and the prevailing flow field conditions, ensuring that the post-reflection movement adheres to physical principles.

2.4. Shoreline, Water Depth, and COD Data

The shoreline data were derived from remote sensing images, extracted according to the mean spring tides high tide line, and appropriately adjusted according to the accuracy of the model grid. The bathymetry data were obtained from the nautical charts published by the Department of Navigation Protection of the Chinese People's Liberation Army and the DHI C-MAP. The COD data were from the WQ data released by the National Seawater Quality Monitoring Information Public System of the Ministry of Ecology and Environment of the People's Republic of China, monitored in the autumn of 2021 (October and November) by the National Marine Environment Monitoring Center.

3. Results

3.1. COD Concentration Monitoring Results

The overall COD concentration in Liaodong Bay in autumn of 2021 shows a higher concentration in the estuarine region and gradually decreases toward the sea. It can be seen from Figure 2 that the highest COD concentration is 4.9 mg/L in the area between the Liao River and Daliao River, which is 5~6 times higher than the concentration of COD in the mouth of the bay and the center of Liaodong Bay. This shows that Liao River and Daliao River in Liaodong Bay are the main pollution sources in terms of COD in Liaodong Bay. The COD concentration decreases with the distance from the mouth of the rivers, but the contour plot of the COD concentration shows that there are also COD areas with a higher concentration far from the estuary (regions in the figure with COD concentrations above 3.5 mg/L) in the north side of Dalian and west side of Yingkou. This appears anomalous against the background of COD degradation over time.

3.2. MIKE21 Model Verification

In this paper, the model is calibrated using current data measured at 10 stations, as shown in Figure 3. These data, including velocity and flow direction, are from the observation results of Tianjin Survey and Design Institute for Water Transport Engineering Co., Ltd., in Liaodong Bay from 18 September to 19 September 2021. The sea current observations were carried out using an acoustic Doppler current profiler, with the water column divided into six vertical layers. The equipment underwent a self-check before the observations. The model started at 00:00 on 15 September 2021. The initial conditions set the water level and velocity field to zero. The time step for the open boundary water-level conditions is one hour, which includes the seasonal variations in the water level. The comparisons between the model-calculated data and the measured data for all stations are shown in Figure 4. The validation results indicate that the model-calculated values and the measured values of flow velocity and direction are relatively consistent across all stations. The range of the average flow velocity error is between 0.01 and 0.11 m/s, and the average flow direction deviation is between 0.16° and 19.76°, with the error values within a reasonable range. The discrepancies between simulated and observed tidal current values may be attributed to observational errors, as well as non-linear effects, such as topography and bottom friction. From the comparison results, it can be seen that the numerical model can effectively represent the tidal current field in Liaodong Bay and can be used as a basic model for further research work.

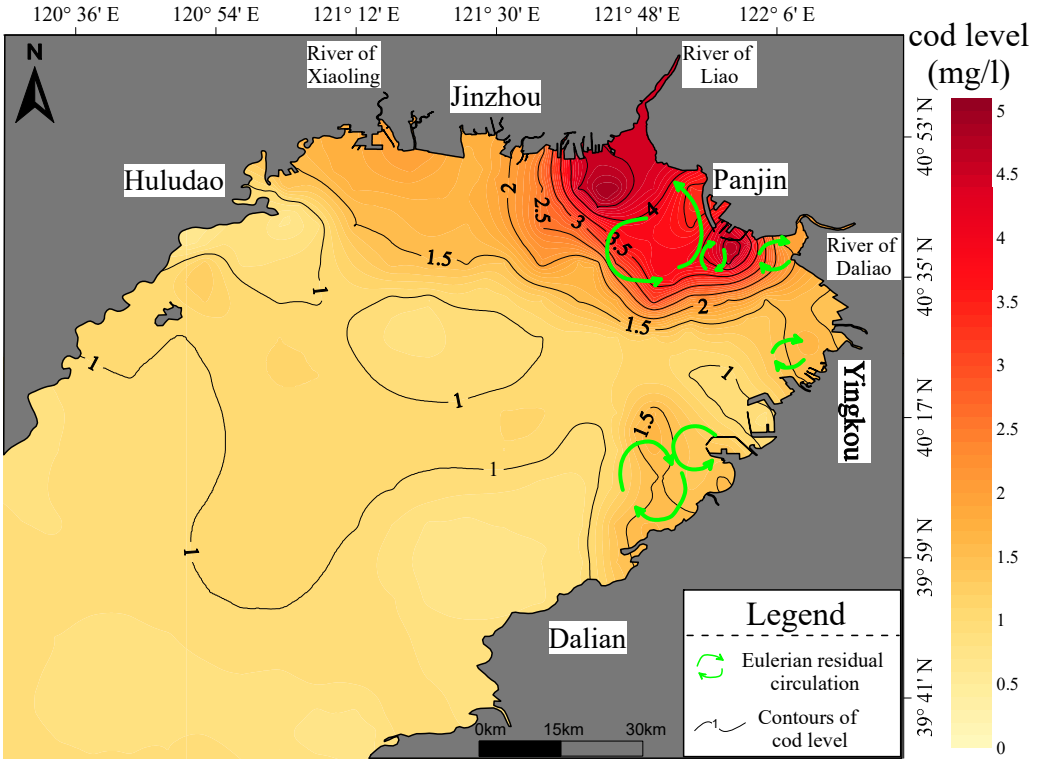

Figure 2. Distribution of COD concentration in Liaodong Bay in autumn 2021.

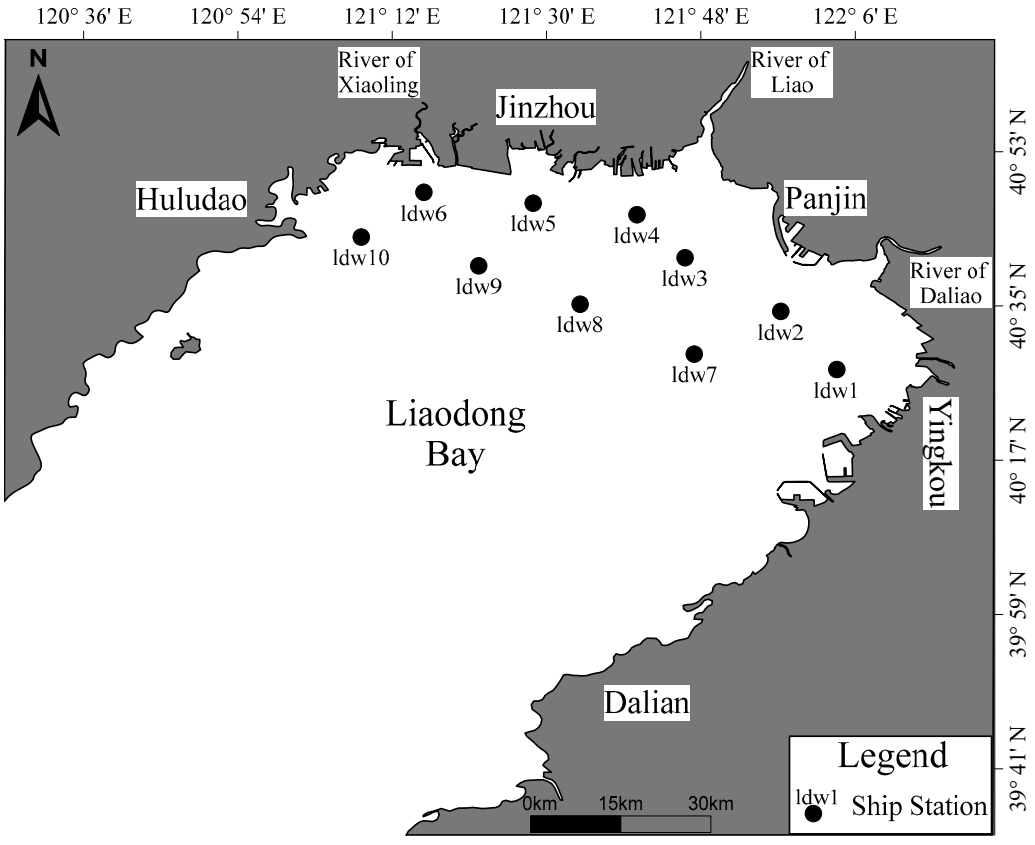

Figure 3. Current observation location.

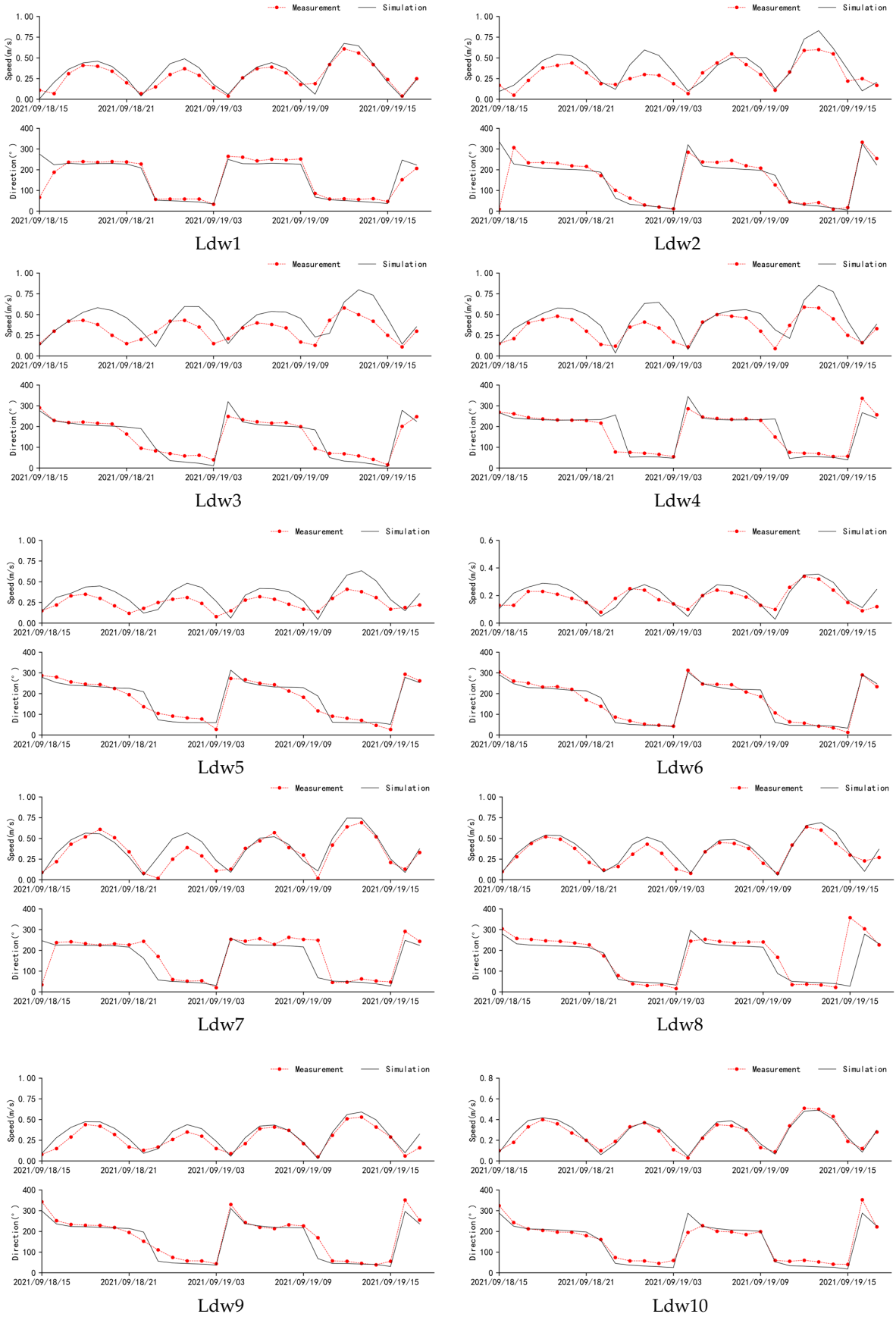

Figure 4. Comparison between calculated and measured data.

3.3. Liaodong Bay Tidal Current

The TC field of Liaodong Bay at the time of the flood tide and ebb tide can be calculated (Figure 5). At the time of the flood tide, the water flows from the Bohai Sea to the bay and converges at the estuary of the Liao River; the TC velocity gradually increases from the mouth of the bay to the estuary, and the maximum TC velocity is about 0.2 m/s at the mouth of the bay, 0.3 m/s in the central area of Liaodong Bay, and about 0.9 m/s at the estuary of the Liao River. During the ebb tide, the TC flows from Liaodong Bay to the Bohai Sea, contrary to the time of the flood tide, the maximum TC velocity is about 0.3 m/s at the estuary of the Liao River, 0.5 m/s at the center of Liaodong Bay, and 0.6 m/s at the mouth of the bay.

3.4. Euler Residual Current

Based on the calculated TC field and the definition of ERC in Section 2.2, taking 750 h (15 October to 15 November 2021) as the averaging time, this paper calculated the ERC field of Liaodong Bay for the same period as the COD observations, as shown in Figure 6. The ERC in Liaodong Bay is larger in the nearshore and estuary regions, and smaller in the central region of Liaodong Bay, which is also consistent with the mechanism of ERC caused by the non-linear effects of the shoreline. In addition, the distribution of the circulation is also a distinctive feature of the ERC field in Liaodong Bay, especially in the estuarine area at the north and the east coast of Liaodong Bay. There is a circulation current in the Liao River estuary near the west side of Panjin, the south side of Panjin, and the estuary of Daliao River, in the counterclockwise, clockwise, and clockwise direction, respectively, and with ERC velocities ranging from 0.02 to 0.1 m/s. Between the city of Dalian and Yingkou on the east coast of Liaodong Bay, three circulation currents also exist from south to north, in clockwise, counterclockwise, and clockwise directions, and with ERC velocities ranging from 0.01 to 0.3 m/s.

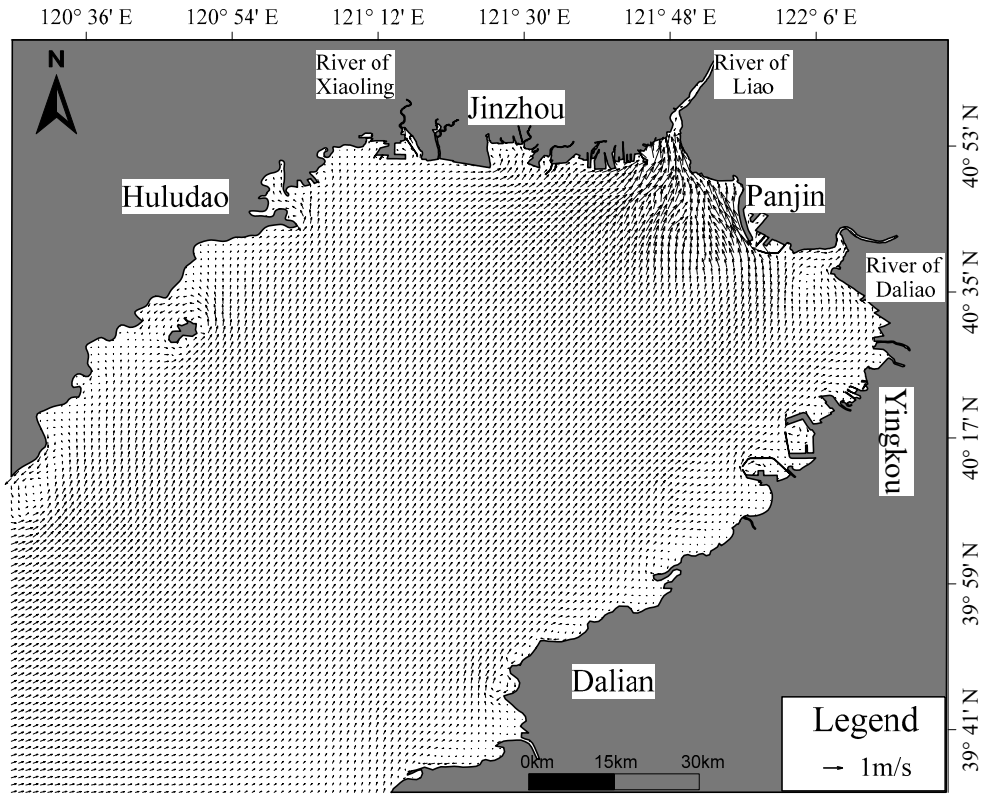

(**a**) Flood tide

Figure 5. *Cont.*

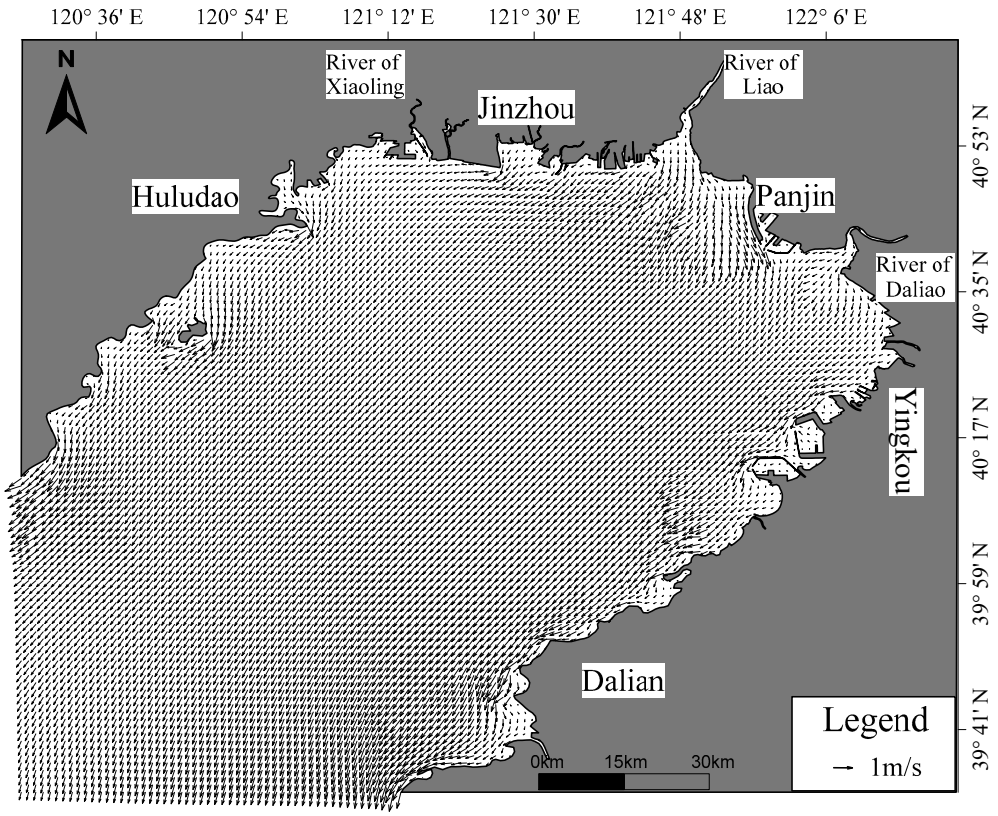

(**b**) Ebb tide

Figure 5. TC field in Liaodong Bay.

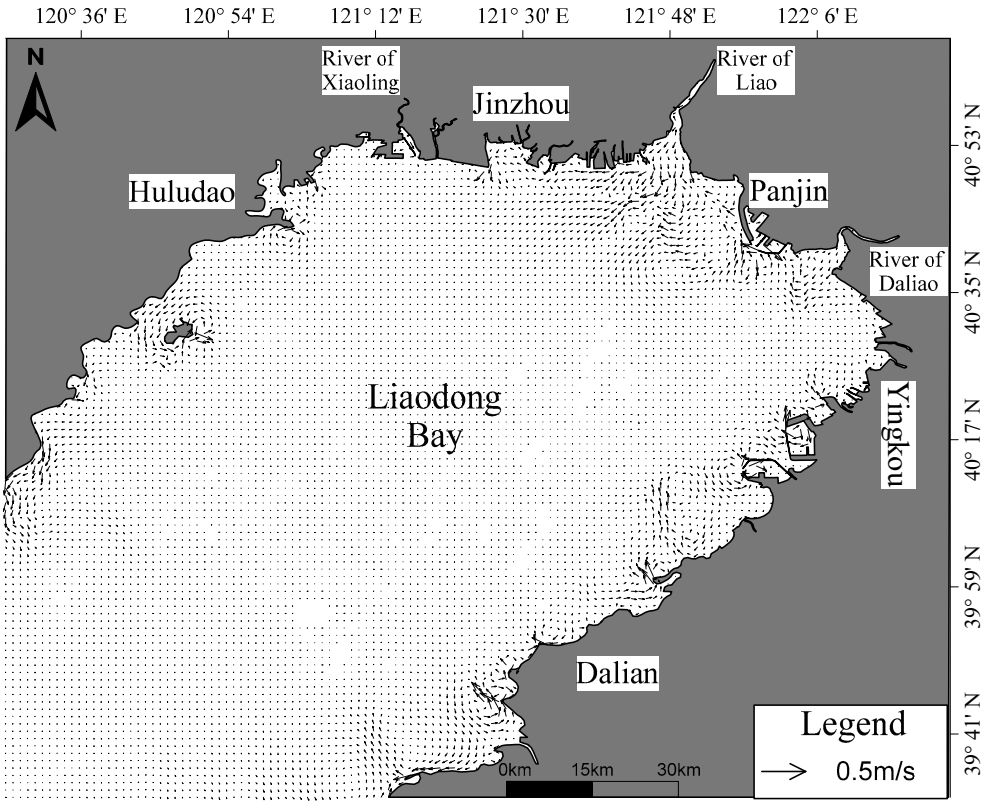

Figure 6. ERC field in Liaodong Bay.

3.5. Lagrangian Residual Current

According to the method introduced in Section 2.2, the LRC field in Liaodong Bay is calculated, and the results are shown in Figure 7. The calculated results of the LRC and ERC are similar, and the LRC velocity in the nearshore and estuarine regions was greater than that in the central region. The LRC velocity in the estuarine region of the Liao River and the Daliao River is between 0.05~0.1 m/s. The maximum velocity on the east coast of Liaodong Bay is about 0.2 m/s. There is also an area of relatively high current velocity, around 0.12 m/s, between the islands south of Huludao and the coastline. LRC flows from the two estuaries to Jinzhou and the Xiaoling River at the top of the bay, and the current velocity gradually decreases. The LRC on the west coast of Liaodong Bay flows along the shoreline to the Bohai Sea, while on the east coast the opposite happens, flowing from Dalian to Yingkou and finally flowing to the two estuary areas of the Liao River and the Daliao River. In addition, one of the distinctive features of the LRC, along the east coast of Liaodong Bay, is that there are several circulations with different radii and flow velocities in the nearshore area.

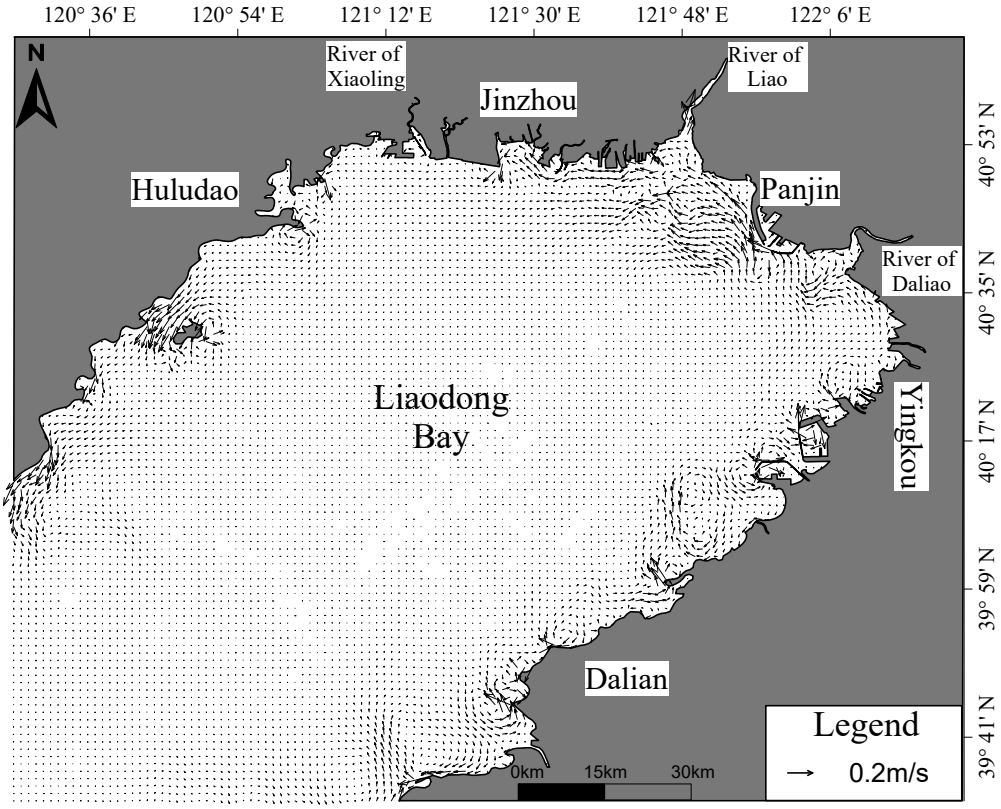

Figure 7. LRC field in Liaodong Bay.

3.6. Particle Tracking

The positions and displacements of uniformly distributed particles in Liaodong Bay, after 750 h, for the calculated TC, are given in Figure 8. After 750 h under the influence of the TC, uniformly distributed free particles in the two river estuaries and adjacent sea areas mostly migrate toward the center of the bay. Meanwhile, the particle displacement after 750 h indicates that the particle displacement in the two estuaries and near the shore is larger than that in the center of Liaodong Bay. In addition, the displacement of particles on the east coast of Liaodong Bay points to the two estuaries, while that in the two estuaries points to the Xiaoling estuary and the sea near Huludao on the west coast, and the displacement of particles is inversely proportional to the distance from the two estuaries, namely the farther away from the river mouth, the smaller the displacement.

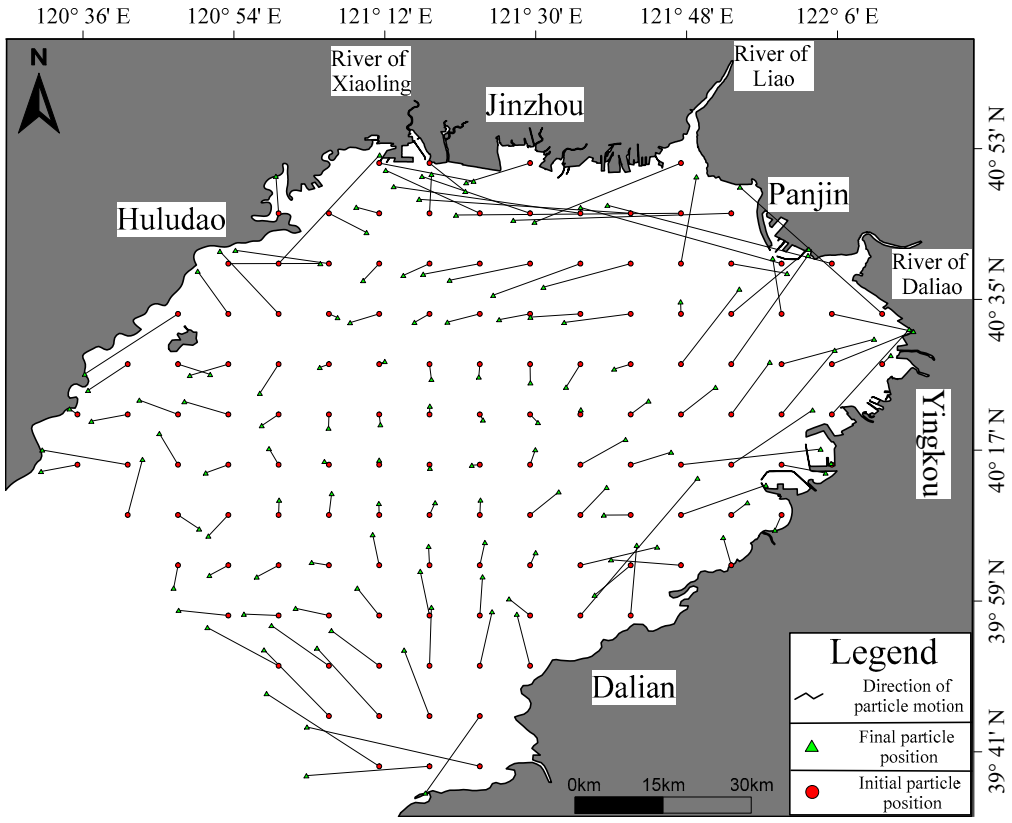

Figure 8. Particle tracking results in Liaodong Bay.

4. Discussion

The COD concentration distribution in Liaodong Bay show that the Liao River and the Daliao River, as the main sea-entering rivers in Liaodong Bay, are the main sources of COD pollution in Liaodong Bay. The pollutants originating from the rivers spread to all parts of the bay under the flow of tidal currents. Therefore, it is crucial to fully understand the hydrodynamic process of Liaodong Bay and analyze the dynamic mechanisms of pollutant transportation to solve the transportation problem of riverine COD into Liaodong Bay. This article compares the COD observation results with the calculated Euler residual current, Lagrangian residual current, and particle tracking results, to explore the hydrodynamic mechanisms behind pollutant transportation represented by COD.

4.1. COD and Euler Residual Current

Figures 2 and 6 show that there is good agreement between the COD concentration distribution and ERC circulation. The COD concentration at the monitoring stations between the Liao River and Daliao River estuaries is the highest in Liaodong Bay, and there are also three circulations of different sizes in the ERC field here. This overlap is partly due to the fact that the Liao River and the Daliao River are the main sources of COD in Liaodong Bay; the ERC plays a noteworthy role in causing a significant amount of COD to be retained in this area. At the same time, there are three ERCs with a slightly smaller radius in the east coast of Liaodong Bay away from the estuaries, and the COD concentration in the center of the currents and the neighboring areas is obviously higher than that of the surrounding stations. This indicates that the ERC circulation has a certain impact on the distribution of COD. In the central area of the circulation, the recirculation of COD within this area results in a lower diffusion rate compared to the surrounding sea areas, making it easy to form COD hotspots, with concentrations higher than the background level. The conclusion by Kong is consistent with the findings of this study [29].

4.2. Lagrangian Residual Current and COD

The ERC circulation has a certain impact on local COD hotspots, while the influence of LRC on COD distribution is manifested in long-distance transportation. The area with >1.5 mg/L COD, in Figure 2, shows that the COD in this concentration range is mainly distributed in the west side of the two estuaries, which indicates that the COD is mainly transported to the west bank of Liaodong Bay after leaving the estuarine region. Because the COD concentration in this area is higher than the background value in the middle of the bay and the bay mouth away from the estuary, the contour pattern reflects the gradual reduction in COD from the high concentration area at the source of the two estuaries to the low concentration area in the middle of the bay and the bay mouth, which is a good indication of the direction of pollutant transportation. The flow field of the LRC in the two estuarine regions and the diffusion direction of COD outward from the estuarine region are pretty consistent in Figures 2 and 7, indicating that the LRC plays an important role in the long-distance transportation of COD with a higher concentration than the background concentration, and it can effectively indicate the transportation direction of substances.

4.3. Particle Tracking and COD Transport

Comparing the COD concentration distribution and the PT results, there are two findings. Firstly, the ending position and distribution density of the particles after drifting for 750 h under the action of TC largely explains the COD concentration distribution; Figure 8 shows that the particle density in the western part of the two estuaries is generally higher than that in the eastern part, which is consistent with the fact that the COD concentration shows a higher value in the west than in the east of the estuaries, according to the analysis in Section 4.2. Meanwhile, the final position of most of the particles from the river estuaries and adjacent coastal areas are predominantly located in the central part of Liaodong Bay, which is consistent with the fundamental understanding of COD transportation from river estuaries into the inner Liaodong Bay. Secondly, the displacement of the particles, as shown in Figure 8, is a key factor that provides the transportation process of the substances in the region with a vector and has a good level of representation in terms of the direction and capacity of COD transportation in various places in the bay. This result is verified by the COD transportation process from the two estuaries to the western part of the sea. Moreover, due to the influence of stochastic terms in the PT results, the magnitude of particle displacement is more significant than its direction. The magnitude of particle displacement can be considered as an indicator of the bay's material transportation capacity. However, in the area near the mouths of the two rivers, where TCs are strong, the direction of particle displacement is relatively consistent, which can also indicate the direction of material transportation.

5. Conclusions

In this paper, a numerical model verified by measured current data was established in the Bohai Sea, China. The TC, ERC, LRC, and PT in Liaodong Bay and the Bohai Sea were calculated through the numerical model, and the concentration distribution and transportation pattern of COD, monitored during the same period, were analyzed from the perspective of hydrodynamic mechanisms. The following findings were made:

(1) COD in Liaodong Bay has highest concentration in the estuary of the Liao River and the Daliao River and the surrounding areas, and the concentration gradually decreases from the two estuaries to the sea. The distribution of the area with >1.5 mg/L COD in the east coast and west coast differs. Overall, the west coast has more area with >1.5 mg/L COD than the east coast, but there is also a local high concentration area between Dalian and Yingkou in this area;

(2) The COD enrichment area between the Liao River and the Daliao River and on the east coast is consistent with the distribution of the ERC circulation, the recirculation of COD within this area results in a lower diffusion rate compared to the surrounding

sea areas, making it easy to form COD hotspots, with concentrations higher than the background level;

(3) The LRC mainly influences the overall long-distance transportation of COD and plays a dominant role in the transportation of COD with a concentration that is higher than the background value in the center of the bay, but less than the peak concentration in the estuarine regions. The direction of COD transportation, indicated by the 1.5 mg/L~2 mg/L COD contour pattern, is consistent with the flow velocity and direction of the LRC field in the same region;

(4) The displacement of the particles from the initial and final position can be used as a scalar to indicate the transportation capacity of different regions of the bay. The end position and distribution density of the particles can indicate the distribution characteristics of COD after leaving the estuarine regions. The final position of the particles is mainly concentrated in the central and west side of the bay, which is consistent with the common knowledge on COD transportation from the estuary to the sea and the main transportation direction analyzed in this paper.

Author Contributions: Methodology, Software, Writing—Original draft preparation, X.L.; Writing—Review & Editing, J.D., L.Z., G.Z., X.D. and J.S.; Conceptualization, Data curation, Investigation, P.W.; Funding acquisition, G.Z. All authors have read and agreed to the published version of the manuscript.

Funding: This work was supported by the National Key Research and Development Program of China (2023YFC3208400)] and the National Natural Science Foundation of China [Grant No. 42201070].

Data Availability Statement: The original contributions presented in the study are included in the article, further inquiries can be directed to the corresponding author.

Conflicts of Interest: The authors have no relevant financial or non-financial interests to disclose.

References

1. Wei, H.; Sun, J.; Moll, A.; Zhao, L. Phytoplankton dynamics in the Bohai Sea—Observations and modelling. *J. Mar. Syst.* **2004**, *44*, 233–251. [CrossRef]
2. Li, K.; Ma, Y.; Dai, A.; Wang, X. Degradation dynamics and bioavailability of land-based dissolved organic nitrogen in the Bohai Sea: Linking experiment with modeling. *Mar. Pollut. Bull.* **2017**, *124*, 856–870. [CrossRef] [PubMed]
3. Chen, C.; Liang, J.; Yang, G.; Sun, W. Spatio-temporal distribution of harmful algal blooms and their correlations with marine hydrological elements in offshore areas, China. *Ocean Coast. Manag.* **2023**, *238*, 106554. [CrossRef]
4. Yang, H.F.; Zhu, Q.Y.; Liu, J.A.; Zhang, Z.L.; Yang, S.L.; Shi, B.W.; Zhang, W.X.; Wang, Y.P. Historic changes in nutrient fluxes from the Yangtze River to the sea: Recent response to catchment regulation and potential linkage to maritime red tides. *J. Hydrol.* **2023**, *617*, 129024. [CrossRef]
5. Gajardo, G.; Morón-López, J.; Vergara, K.; Ueki, S.; Guzmán, L.; Espinoza-González, O.; Sandoval, A.; Fuenzalida, G.; Murillo, A.A.; Riquelme, C.; et al. The holobiome of marine harmful algal blooms (HABs): A novel ecosystem-based approach for implementing predictive capabilities and managing decisions. *Environ. Sci. Policy* **2023**, *143*, 44–54. [CrossRef]
6. Wang, K.; Wei, Q.; Jian, H.; Gao, Z.; Yao, Q. Variations in the nutrient concentration and composition in Liaodong Bay under long-term human activities. *Mar. Pollut. Bull.* **2022**, *182*, 114016. [CrossRef] [PubMed]
7. Kong, X.; Ye, S. The impact of water temperature on water quality indexes in north of Liaodong Bay. *Mar. Pollut. Bull.* **2014**, *80*, 245–249. [CrossRef]
8. Dai, A.; Li, K.; Ding, D.; Li, Y.; Liang, S.; Li, Y.; Su, Y.; Wang, X. Total maximum allocated load calculation of nitrogen pollutants by linking a 3D biogeochemical–hydrodynamic model with a programming model in Bohai Sea. *Cont. Shelf Res.* **2015**, *111*, 197–210. [CrossRef]
9. Yang, F.; Su, R.; Jian, H.; Yao, Q. Using algal biomass to evaluate numeric nutrient criteria in an estuary: A case study of Daliaohe Estuary in China. *Ecol. Indic.* **2016**, *70*, 373–381. [CrossRef]
10. Ghaemi, M.; Mohammadpour, G.; Hamzei, S.; Gholamipour, S. Spatial and temporal characterizations of seawater quality on marine waters area of the Persian Gulf. *Reg. Stud. Mar. Sci.* **2022**, *53*, 102407. [CrossRef]
11. Lega, M.; Kosmatka, J.; Casazza, M.; De Maio, L.; Severino, D.; Teta, R. Environmental monitoring and assessment: A multi-scale and multiparameter case study in Campania Region (S Italy) on the recreational seawater quality evaluation. *Reg. Stud. Mar. Sci.* **2020**, *39*, 101465. [CrossRef]
12. Li, X.; Lei, G.; Li, Y.; Wang, Y.; Tan, Z. Assessing hydrodynamic effects of ecological restoration scenarios for a tidal-dominated wetland in Liaodong Bay (China). *Sci. Total Environ.* **2021**, *752*, 142339. [CrossRef]

13. Wei, H.; Hainbucher, D.; Pohlmann, T.; Feng, S.; Suendermann, J. Tidal-induced Lagrangian and Eulerian mean circulation in the Bohai Sea. *J. Mar. Syst.* **2004**, *44*, 141–151. [CrossRef]
14. Yang, S.; Li, J.; Ye, S.; Mackenzie, L.; Yuan, H.; He, L.; Zhao, G.; Pei, S.; Ding, X. Pollen distribution and transportation patterns in surface sediments of Liaodong Bay, China. *Sci. Total Environ.* **2021**, *771*, 144883. [CrossRef]
15. Zhang, C.; Lei, M.; Liu, X.; Zhou, Z.; Liu, M.; Chen, H.; Yang, W.; Wang, X. Presence and inputs of legacy and novel per- and polyfluoroalkyl substances from rivers and drainage outlets to Liaodong Bay, China. *Reg. Stud. Mar. Sci.* **2022**, *56*, 102684. [CrossRef]
16. Wu, J.; Wang, Z.; Tian, J.; Wang, K.; Li, A.; Li, N.; Song, L.; Song, G. Comparison of nutrients status in Liaodong Bay and Northern Yellow Sea, China: Controlling factors and nutrient budgets. *Mar. Environ. Res.* **2024**, *194*, 106338. [CrossRef]
17. Xu, Y.; Gao, H.; Li, R.; Lou, Y.; Li, B.; Cheng, G.; Na, G. Occurrence and distribution of antibiotics and antibiotic resistance genes from the land to ocean in Daliao River-Liaodong Bay, China. *Mar. Environ. Res.* **2024**, *197*, 106470. [CrossRef]
18. Ye, Y.; Zhang, A.; Teng, J.; Yang, X.; Yuan, X.; Wang, Q.; Zhao, J.; Zhang, B.; Zhang, T.; Chen, X.; et al. Pollution characteristics and ecological risk of microplastic in sediments of Liaodong Bay from the northern Bohai Sea in China. *Mar. Pollut. Bull.* **2023**, *187*, 114505. [CrossRef]
19. Luo, M.; Zhang, Y.; Xiao, K.; Wang, X.; Zhang, X.; Li, G.; Li, H. Effect of submarine groundwater discharge on nutrient distribution and eutrophication in Liaodong Bay, China. *Water Res.* **2023**, *247*, 120732. [CrossRef] [PubMed]
20. Pei, S.; Laws, E.A.; Zhu, Y.; Zhang, H.; Ye, S.; Yuan, H.; Ding, X. Nutrient dynamics and their interaction with phytoplankton growth during autumn in Liaodong Bay, China. *Cont. Shelf Res.* **2019**, *186*, 34–47. [CrossRef]
21. Ma, Q.; Liang, S.; Sun, Z.; Zhang, R.; Wang, P. Development and evaluation of a GPU-based coupled three-dimensional hydrodynamic and water quality model. *Mar. Pollut. Bull.* **2023**, *187*, 114494. [CrossRef] [PubMed]
22. Liu, H.; Yin, B. Numerical investigation of nutrient limitations in the Bohai Sea. *Mar. Environ. Res.* **2010**, *70*, 308–317. [CrossRef] [PubMed]
23. Wang, P.; Zhang, L.; Lin, X.; Yan, J.; Zhang, P.; Zhao, B.; Zhang, C.; Yu, Y. Spatial distribution, control factors and sources of heavy metal in the surface sediments of Fudu Estuary waters, East Liaodong Bay, China. *Mar. Pollut. Bull.* **2020**, *156*, 111279. [CrossRef] [PubMed]
24. Zhang, A.; Wang, L.; Zhao, S.; Yang, X.; Zhao, Q.; Zhang, X.; Yuan, X. 2017. Heavy metals in seawater and sediments from the northern Liaodong Bay of China: Levels, distribution and potential risks. *Reg. Stud. Mar. Sci.* **2020**, *11*, 32–42.
25. Wu, J.; Wang, Z.; Zhang, Y.; Tian, J.; Song, L.; Han, J.; Yu, J.; Zhang, Y. Spatial distribution and ecological risks of polycyclic aromatic hydrocarbons in sea ice and seawater from northern Liaodong Bay, China. *Mar. Pollut. Bull.* **2022**, *174*, 113319. [CrossRef] [PubMed]
26. Hou, W.; Chen, X.; Wu, J.; Zhang, C.; Yu, J.; Bai, J.; Chen, T. Sources and spatiotemporal variations of nitrogen and phosphorus in Liaodong Bay, China. *Mar. Pollut. Bull.* **2022**, *185*, 114191. [CrossRef] [PubMed]
27. Rodríguez, P.A.; Carbajal, N.; Rodríguez, J.H.G. Lagrangian trajectories, residual currents and rectification process in the Northern Gulf of California. *Estuar. Coast. Shelf Sci.* **2017**, *194*, 263–275. [CrossRef]
28. Liubartseva, S.; Coppini, G.; Lecci, R.; Creti, S. Regional approach to modeling the transport of floating plastic debris in the Adriatic Sea. *Mar. Pollut. Bull.* **2016**, *103*, 115–127. [CrossRef]
29. Kong, X. Influence of inter-river water diversion on estuary pollution control: A case study of Liaodong Bay. *Reg. Stud. Mar. Sci.* **2024**, *70*, 103362. [CrossRef]

Disclaimer/Publisher's Note: The statements, opinions and data contained in all publications are solely those of the individual author(s) and contributor(s) and not of MDPI and/or the editor(s). MDPI and/or the editor(s) disclaim responsibility for any injury to people or property resulting from any ideas, methods, instructions or products referred to in the content.